ELSEVIER

Cement & Concrete Composites 25 (2003) 607–615

Cement & Concrete Composites

www.elsevier.com/locate/cemconcomp

A probabilistic multiparameter framework for the modeling of fatigue crack growth in concrete

K. Bhalerao [a], W. Shen [b], A.B.O. Soboyejo [a], W.O. Soboyejo [b,*]

[a] Department of Food, Agricultural and Biological Engineering, The Ohio State University, Columbus, OH 43210, USA
[b] Department of Mechanical and Aerospace Engineering, The Princeton Materials Institute, Princeton University, P.O. Box CN 5263, Princeton, NJ 08544-5263, USA

Abstract

This paper presents a probabilistic multiparameter framework for the modeling of fatigue crack growth in three grades of concrete. The framework relies on the use of ranked fatigue crack growth rate data (with specified occurrence probability levels) in the formulation of multiparameter fatigue crack growth expressions. These relate ranked fatigue crack growth rates to crack driving force parameters such as the stress intensity factor range, maximum stress intensity factor, stress ratio and occurrence probability level. A probabilistic framework is then presented for the estimation of material reliability or failure probability due to fatigue crack growth. The probabilistic model is then validated for the available data.

Keywords: Probabilistic; Multiparameter; Modeling; Fatigue; Crack growth; Concrete

1. Introduction

The development of an extensive global network of infrastructure has been achieved largely by the use of concrete [1]. This has stimulated the growth of a trillion-dollar industry that supplies much of the infrastructure materials for pavements, buildings, and oil wells [1]. However, in all these applications, sub-critical crack growth may occur at stress levels that are well below the critical conditions required for failure under monotonic loading [2]. Such sub-critical crack growth is generally associated with cyclic loading due to freeze–thaw cycles [3], mechanical loading by traffic, and wind loading on structures. These cyclic loads can give rise to fatigue crack growth processes [2,4] that may be exacerbated by the additional effects of the environment [5].

The analysis of fatigue crack growth in concrete is complicated by the heterogeneous nature of concrete. Depending on the local combinations of sand, cement and aggregate, this may give rise to significant variations in fatigue crack growth rates within any given mix of concrete. This suggests that a statistical/probabilistic framework is needed for the modeling of crack growth in concrete. Furthermore, a wide range of parameters may influence fatigue crack growth rates in concrete. These include mechanical parameters such as: the stress intensity factor range, stress ratio and the maximum stress intensity factor. Fatigue crack growth rates may also be influenced by environmental parameters such as relative humidity and temperature, which are not considered in this paper.

This paper presents a multiparameter framework for the probabilistic fracture mechanics modeling of fatigue crack growth in concrete. The approach is demonstrated for three concrete mixes with strengths of 30, 35 and 40 MPa. The "scatter" in the fatigue crack growth rate data is shown to be well characterized by log-normal statistical distribution. Fatigue crack growth rates at specific probability levels are also shown to be well described by multiparameter fracture mechanics expressions that relate the measured fatigue crack growth rates to the stress intensity factor range, stress ratio, maximum stress intensity factor and occurrence probability. The fracture mechanics expressions are then used as inputs into a probabilistic framework for the estimation of crack growth rates associated with specified probability levels. Finally, the implications of the results are

* Corresponding author. Tel.: +1-609-258-5609; fax: +1-609-258-5877.
E-mail address: soboyejo@princeton.edu (W.O. Soboyejo).

0958-9465/02/$ - see front matter © 2002 Published by Elsevier Science Ltd.
doi:10.1016/S0958-9465(02)00074-4

discussed for the design of concrete infrastructure with improved fatigue resistance.

2. Design of concrete specimens

The composition of the three types of concrete that were used in this study is summarized in Table 1. These were obtained from Ref. [6], which specifies the compositions for the mixing of concrete with strength levels of 30, 35 and 40 MPa. The three types of concrete were prepared at the Ohio State University, Columbus, OH. The concrete mixes did not use any admixtures. 204 mm long single edge notched bend (SENB) specimens with rectangular cross-sections (51 mm × 51 mm) were cast for subsequent fatigue crack growth experiments. The specimen dimensions were carefully selected to be similar to those used by Bazant and Xu in prior work [7]. Ordinary Portland cement—Type I was used in the concrete mix. The sand used in the mix was finer than 4.75 mm and the coarse aggregate was irregular river gravel, commercially available in the Columbus, OH region. The coarse aggregate size ranged from 10 to 12 mm. The mix was poured into plywood moulds and tamped with a steel rod to remove any voids. The microstructures of the cured specimens are presented in Fig. 1a–c.

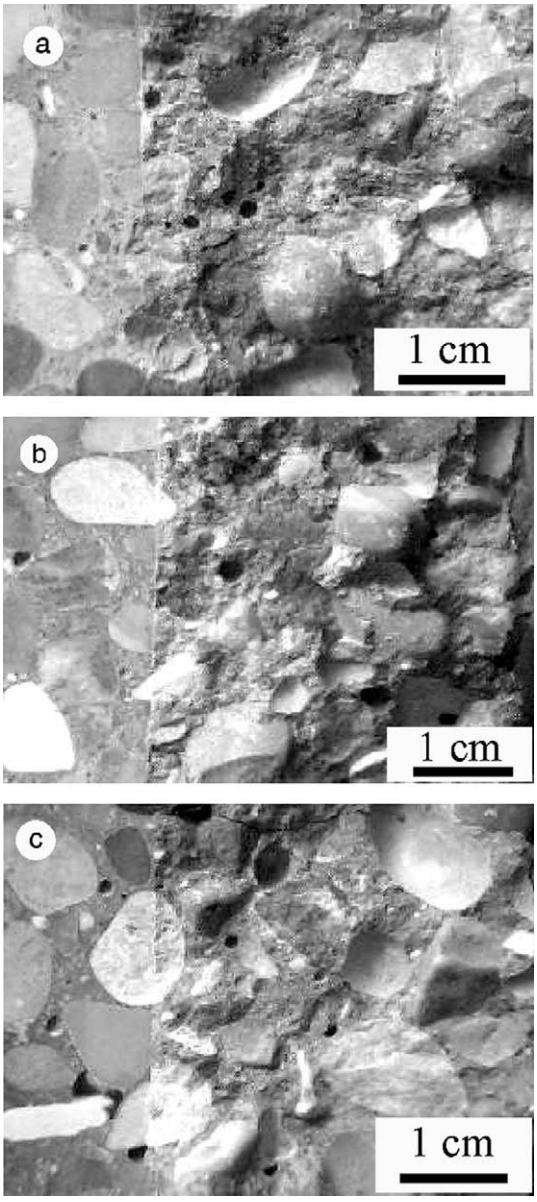

Fig. 1. Microstructure of the three types of concrete with strength levels of: (a) 30 MPa, (b) 35 MPa and (c) 40 MPa.

3. Experimental procedures

The cast concrete blocks were cured under water for at least 30 days. After this period, notches were introduced into the blocks using 1.02 mm thick diamond wheels that were mounted on a sliding fixture that facilitated the introduction of 1.02 mm wide notches with well-controlled notch profiles and orientations. In this way, SENB specimens with notch-to-width ratios of about 0.25 were produced for subsequent fatigue crack growth testing.

The fatigue crack growth experiments were carried out in a computer-controlled Instron servo-hydraulic testing machine (Instron, Canton, MA). Crack growth was monitored using a Questar telescope and a clip gauge that was attached to the notch mouth using knife edges. Initial stress intensity factor ranges of 0.3 $MPa\sqrt{m}$ (about 0.45 kN) were applied to the specimen,

Table 1
Composition of the three types of concrete (Erntroy and Shacklock method for high strength concrete design)

	Mix (30 MPa)	Mix (35 MPa)	Mix (40 MPa)
Cement	Type I; 1 part; 456.59 kg/m^3	Type I; 1 part; 513.39 kg/m^3	Type I; 1 part; 609.26 kg/m^3
Coarse aggregate	Irregular gravel; 2.672 parts; 1220.23 kg/m^3	Irregular gravel; 2.255 parts; 1172.42 kg/m^3	Irregular gravel; 1.808 parts; 1101.57 kg/m^3
Fine aggregate	Well-graded sand; 0.890 parts; 406.74 kg/m^3	Well-graded sand; 0.751 parts; 390.47 kg/m^3	Well-graded sand; 0.602 parts; 360.19 kg/m^3
Workability	Medium	Medium	Medium
Water/cement ratio	0.416; 190.18 l/m^3	0.378; 196.84 l/m^3	0.338; 206.37 l/m^3

and were increased in 5–10% steps until stable crack growth was detected by the notch-mouth clip gauge (compliance technique) after 10,000–50,000 cycles. A steady increase in the value of the compliance over time indicates steady crack growth. The load ranges were then maintained constant, as the crack length increased beyond the near-fatigue-threshold regime. Most of the tests were continued until specimen fracture occurred. However, in selected cases, the tests were stopped prior to specimen failure. This was done to facilitate a study of the interactions of the crack with the underlying concrete microstructure.

The fatigue crack growth rate tests were performed at stress ratios, $R = K_{min}/K_{max}$, of 0.1, 0.25 and 0.5, where K_{min} and K_{max} are the minimum and maximum stress intensity factors applied to the specimen. One specimen of each grade was tested at one R ratio. All the tests were conducted at room temperature in laboratory air with a relative humidity of 40%. A cyclic frequency of 10 Hz was used. Also, after specimen failure (fracture), the fracture surfaces of selected specimens were coated with a few nanometers of gold, and examined under a scanning electron microscope. The cyclic fracture modes were thus compared to the monotonic fracture modes obtained from separate experiments on the same materials.

4. Results and discussion

4.1. Fatigue crack growth rates

A summary of the fatigue crack growth rate data obtained from the current study is presented in Fig. 2a–c. These show data obtained for stress ratios, R, of 0.1, 0.25 and 0.5, respectively. The data exhibit significant scatter, which is consistent with the heterogeneous structure of the concrete materials that were studied. Also, the wide scatter in the plots of fatigue crack growth rate versus stress intensity factor range suggests that the crack growth rates cannot be analyzed simply within a deterministic framework.

The measured fatigue crack growth rate data were, therefore, statistically ranked, for specified stress intensity factor ranges. In this way, statistical distributions of fatigue crack growth rates were obtained for stress intensity factor ranges of 0.58, 0.61, 0.67, and 0.71 MPa$\sqrt{m}$. Typical results obtained from the ranking process are shown in Fig. 3a–d for the concrete mix with a strength of 35 MPa that was tested at a stress ratio, R, of 0.25. The form of the distributions suggests a log-normal distribution of fatigue crack growth rate. This was confirmed with a Kolmogorov–Smirnov (K–S) [11] test that indicated goodness of fit with $P < 0.093$ in all cases.

The log-normal parameters are summarized in Table 2a–c, along with the results of the K–S test for each type

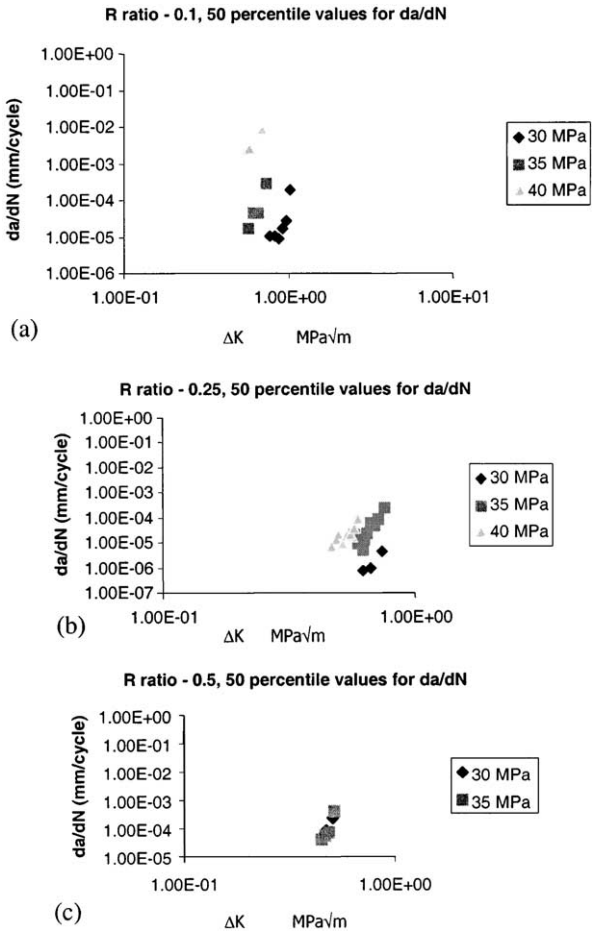

Fig. 2. Summary of fatigue crack growth rate data: (a) $R = 0.1$, (b) $R = 0.3$ and (c) $R = 0.5$.

of concrete. In all cases, the log-normal distribution provides a good fit to the measured variability in the fatigue crack growth rate data. This is consistent with the results of prior work that has shown the variabilities in fatigue crack growth rates in Ti–6Al–4V [8] and gamma titanium aluminide intermetallics [9] are well characterized by log-normal distributions.

It is important to note here that the statistical plots presented in Fig. 2a–c correspond to occurrence probabilities or probability density functions (p.d.f.s.). They may, therefore, be used to identify fatigue crack growth rates associated with specified probability levels. In the current work, fatigue crack growth rate data were identified for p.d.f.s. of 0.05, 0.25, 0.50, 0.75 and 0.95. These were then fitted to multiparameter fracture mechanics expressions that will be presented in Sections 4.2–4.4.

4.2. Multiparameter fatigue crack growth models

The dependence of fatigue crack growth rate, da/dN, on crack driving force is often modeled using the Paris–Erdogan law [10]. This gives:

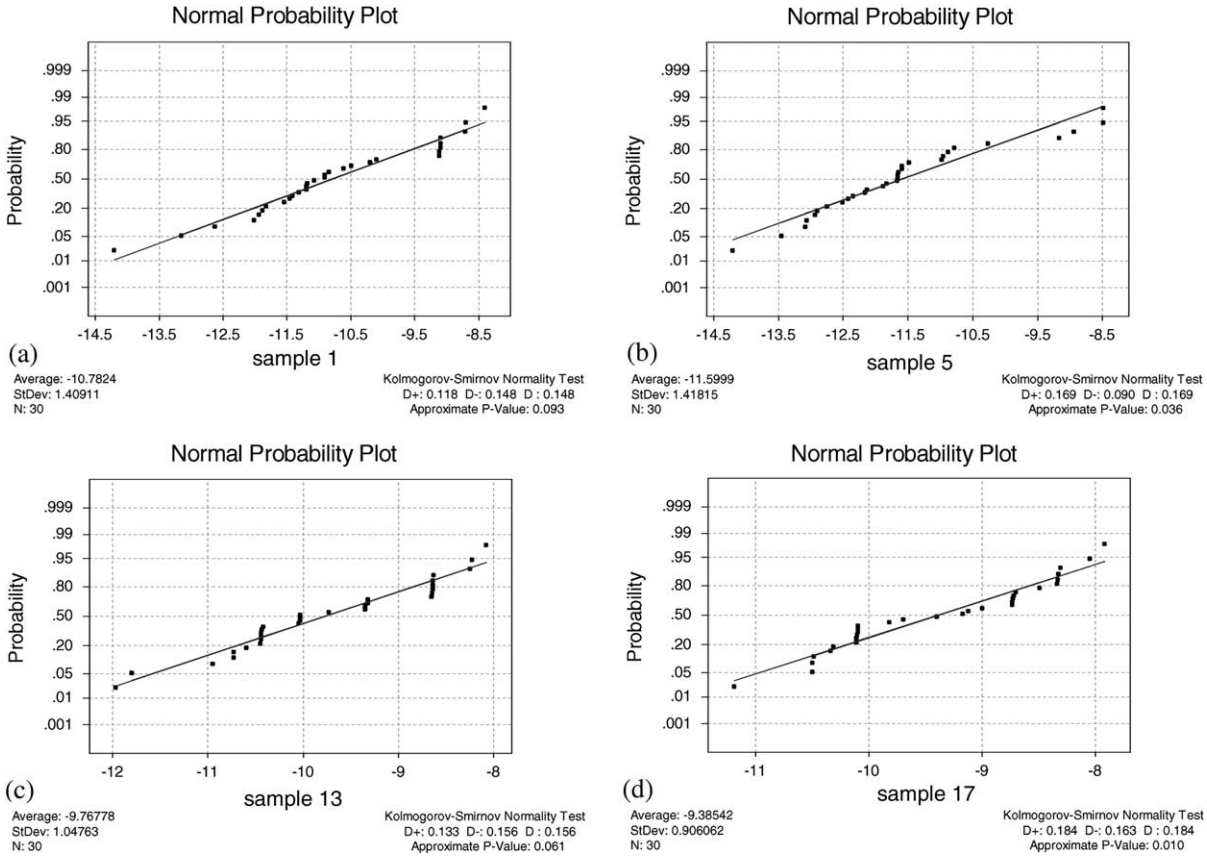

Fig. 3. Summary of variabilities in fatigue crack growth rate data obtained for 35 MPa concrete at stress ratios of 0.25 (a) 0.575 MPa$\sqrt{\text{m}}$, (b) 0.611 MPa$\sqrt{\text{m}}$, (c) 0.665 MPa$\sqrt{\text{m}}$ and (d) 0.71 MPa$\sqrt{\text{m}}$.

$$\frac{da}{dN} = A(\Delta K)^m \tag{1}$$

where A is the Paris coefficient, m is the Paris exponent, and ΔK is the stress intensity factor range. However, in many cases, a single crack driving force, such as ΔK, may not adequately account for all the parameters that influence fatigue crack growth. Hence, it is common to express the fatigue crack growth rate, da/dN, as functions of at least two parameters [9]. The most commonly used two parameter law is:

$$\frac{da}{dN} = A(\Delta K)^m (K_{\max})^n \tag{2}$$

where A, m and n are empirical constants, ΔK is the stress intensity factor range, and $K_{\max}$ is the maximum stress intensity factor range. In the case of concrete, Bazant and Xu [7] have suggested that specimen size has a strong effect on the measured fatigue crack growth rates. They suggest a relationship of the form:

$$\frac{da}{dN} = K_{\text{If}}\left[\frac{\beta}{1+\beta}\right]^{1/2} \tag{3}$$

where K_{If} is the critical stress intensity fracture in Mode I fracture; β is size factor which is called the brittleness number of the specimen [7].

However, there are also other parameters that can influence the fatigue crack growth rate. These include stress ratio, cyclic frequency, crack closure level, etc. The multiparameter dependence of fatigue crack growth rates has been modeled recently by Soboyejo et al. [9]. They propose a general expression of the form:

$$\frac{da}{dN} = \alpha_0(\Delta K)^{\alpha_1}(K_{\max})^{\alpha_2}(R)^{\alpha_3}(K_{\text{cl}})^{\alpha_4}(f)^{\alpha_5}\cdots(X_n)^{\alpha_n} \tag{4a}$$

or

$$\frac{da}{dN} = \alpha_0\prod_{i=1}^{n} X_i^{\alpha_i} \tag{4b}$$

where $\alpha_1, \alpha_2, \alpha_3, \ldots, \alpha_n$ are empirically derived constants obtained from experimental data, ΔK is the stress intensity factor range, $K_{\max}$ is the maximum stress intensity factor in a given fatigue cycle, R is the stress ratio, K_{cl} is the closure stress intensity factor and X_i is any unspecified variable that contributes to the fatigue crack growth process. The multiparameter fatigue crack growth law has been applied previously to a wide range of materials that include steels, Ti–6Al–4V and Inconel 718 [9].

More importantly, the multiparameter law has been extended to the characterization of fatigue crack growth

Table 2
Summary of log-normal probability parameters for concrete with strength levels

Strength (MPa)	*R* ratio	K–S *P*-level	Avg ln(ΔK) (ln(MPa$\sqrt{\text{m}}$))	ln(da/dN) probability levels (ln(mm/cycle))				
				0.05	0.25	0.5	0.75	0.95
(a) 30 MPa								
30	0.1	0.011	−0.25	−13.68	−12.39	−11.49	−10.69	−9.31
30	0.1	0.018	−0.19	−13.93	−12.5	−11.51	−10.51	−9.08
30	0.1	0.13	−0.14	−14.53	−12.8	−11.66	−10.48	−8.79
30	0.1	<0.01	−0.08	−13.63	−12.08	−11.01	−9.94	−8.39
30	0.1	0.052	−0.03	−12.49	−11.33	−10.53	−9.72	−8.57
30	0.1	0.14	0.03	−10.84	−9.52	−8.6	−7.68	−6.36
30	0.25	0.03	−0.47	−15.91	−14.81	−14.05	−13.28	−12.19
30	0.25	0.1	−0.4	−15.46	−14.49	−13.82	−13.14	−12.17
30	0.25	0.14	−0.3	−14.22	−13.11	−12.34	−11.57	−10.46
30	0.5	0.04	−0.75	−10.91	−10.02	−9.41	−8.8	−7.92
30	0.5	0.09	−0.68	−10.46	−9.22	−8.35	−7.49	−6.42
(b) 35 MPa								
35	0.1	0.07	−0.56	−12.74	−11.69	−10.96	−10.23	−9.18
35	0.1	0.12	−0.49	−11.43	−10.57	−9.98	−9.39	−8.53
35	0.1	0.03	−0.42	−11.72	−10.7	−10	−9.29	−8.27
35	0.1	0.04	−0.32	−10.21	−8.98	−8.13	−7.28	−6.05
35	0.25	0.11	−0.55	−13.06	−11.71	−10.78	−9.84	−8.5
35	0.25	0.1	−0.52	−13.64	−12.46	−11.63	−10.81	−9.62
35	0.25	0.05	−0.49	−13.89	−12.54	−11.6	−10.65	−9.3
35	0.25	0.08	−0.47	−15.25	−13.42	−12.15	−10.88	−9.05
35	0.25	0.01	−0.46	−14.06	−12.41	−11.26	−10.12	−8.47
35	0.25	0.01	−0.44	−12.07	−11.49	−10.65	−9.81	−8.61
35	0.25	0.12	−0.4	−11.46	−10.46	−9.76	−9.07	−8.07
35	0.25	0.09	−0.37	−11.41	−10.52	−9.91	−9.3	−8.41
35	0.25	0.03	−0.34	−10.85	−9.98	−9.38	−8.78	−7.92
35	0.25	0.13	−0.28	−9.91	−8.93	−8.32	−7.71	−6.83
35	0.5	0.15	−0.8	−11.5	−10.7	−10.14	−9.58	−8.78
35	0.5	0.1	−0.76	−11.37	−10.46	−9.83	−9.2	−8.29
35	0.5	0.09	−0.72	−10.87	−10.09	−9.54	−9	−8.22
35	0.5	0.04	−0.66	−10.2	−8.81	−7.84	−6.87	−5.48
(c) 40 MPa								
40	0.1	0.03	−0.55	−7.31	−6.53	−5.99	−5.45	−4.67
40	0.1	0.05	−0.37	−7.03	−5.71	−4.79	−3.87	−2.55
40	0.25	0.03	−0.78	−15.21	−13.21	−11.84	−10.46	−8.47
40	0.25	0.06	−0.73	−14.98	−13.03	−12.26	−11.21	−9.7
40	0.25	0.04	−0.7	−13.75	−12.2	−11.13	−10.06	−8.52
40	0.25	0.12	−0.66	−13.83	−12.54	−11.64	−10.74	−9.45
40	0.25	0.14	−0.62	−12.84	−11.68	−10.87	−10.06	−8.89
40	0.25	0.03	−0.59	−12.95	−11.69	−10.81	−9.94	−8.86
40	0.25	0.05	−0.56	−11.89	−10.88	−10.17	−9.47	−8.46
40	0.25	0.08	−0.52	−10.91	−9.97	−9.31	−8.66	−7.72
40	0.25	0.13	−0.42	−8.82	−7.64	−6.82	−5.99	−4.81

in concrete in the present study. This was accomplished by the use of multiple linear regression modeling of experimental data presented in Table 2. The results of Bazant and Xu [7] (Fig. 4) were also analyzed to show the general applicability of the multiparameter framework. Since these show a dependence of fatigue crack growth rate on ΔK and specimen—size, S, a two parameter law was explored. This gives:

$$\frac{\mathrm{d}a}{\mathrm{d}N} = \alpha_0 \left(\frac{\Delta K_{\mathrm{I}}}{\Delta K_{\mathrm{If}}} \right)^{\alpha_1} (S)^{\alpha_2} \tag{5}$$

By conducting multiple linear regression analyses on the data shown in Fig. 4 (taken from [7]), the values of α_0, α_1, and α_2, were obtained to be −15.8, 10.4 and −4.65 respectively ($r^2 = 0.993$). The results of Bazant and Xu [7] are, therefore, well characterized by a two parameter

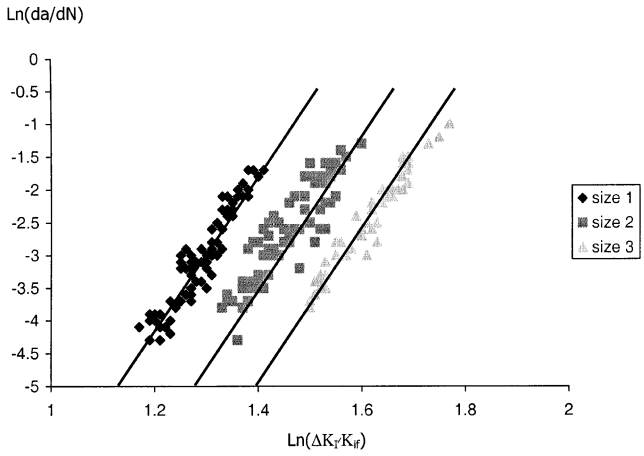

Fig. 4. Bazant and Xu's concrete fatigue crack growth data (taken from Ref. [7]).

law. Furthermore, the relative magnitudes of α_1 and α_2 show the relative contributions from ΔK and specimen size, S, to da/dN.

Due to the measured scatter in the fatigue crack growth rate data obtained from the current study (Fig. 2), a deterministic multiparameter framework was not found to provide an adequate fit to the measured data. A probabilistic fracture mechanics framework was, therefore, developed to include the effects of the statistical scatter/material variability in the analysis of fatigue crack growth. The results from probabilistic fracture mechanics framework are presented below.

4.3. Statistical extension of the multiparameter framework

This section describes the use of ranked statistical data in the determination of functional dependencies between fatigue crack growth rates and multiple variables that include the occurrence probability, ϕ. Hence, the multiparameter law is now expressed as:

$$\frac{da}{dN} = \alpha_0(\Delta K)^{\alpha_1}(K_{max})^{\alpha_2}(R)^{\alpha_3}(\sigma_u)^{\alpha_4}(\phi)^{\alpha_5}\ldots(X_n)^{\alpha_n} \qquad (6)$$

where σ_u is the compressive strength of the concrete, and the other variables have their usual meaning. For simplicity, the dependence of da/dN on ΔK, K_{max} and ϕ is considered. The results are presented in Table 3 for the three types of concrete. In all cases, the multiparameter model provides excellent correlations for values of ϕ of 0.05, 0.25, 0.50, 0.75 and 0.95. Similar correlations are also obtained when R is used instead of K_{max} in the three parameter law. The results are shown in Table 4, which also shows strong correlation between the fatigue crack growth rate data and the selected three variables (ΔK, R and ϕ).

Table 3
Summary of multiparameter constants

CDF	α_0	α_1	α_2	r^2
(a) 30 MPa				
0.05	−12.5	2.44	2.65	0.93
0.25	−11.1	2.96	2.42	0.96
0.5	−10.1	3.83	2.25	0.975
0.75	−9.09	3.86	2.04	0.98
0.95	−7.48	5.18	1.36	0.97
(b) 35 MPa				
0.05	−6.73	10.6	−0.36	0.97
0.25	−7.59	6.20	1.07	0.95
0.5	−7.83	3.94	1.76	0.91
0.75	−8.07	1.7	2.41	0.91
0.95	−7.99	−0.60	3.09	0.84
(c) 40 MPa				
0.05	3.37	27.9	−4.03	0.94
0.25	4.98	30.3	−7.41	0.93
0.5	5.7	30.6	−8.19	0.92
0.75	5.99	29.6	−8.32	0.9
0.95	6.3	27.7	−7.78	0.87

Table 4
Summary of modified multiparameter constants

CDF	α_0	α_1	α_3	r^2
(a) 30 MPa				
0.05	−10.1	4.76	0.985	0.92
0.25	−9.02	5.24	0.823	0.95
0.5	−8.26	5.62	0.704	0.963
0.75	−7.5	6.04	0.573	0.97
0.95	−6.6	6.97	0.223	0.96
(b) 35 MPa				
0.05	−6.93	11.2	−0.4	0.97
0.25	−6.59	8.57	−0.006	0.95
0.5	−6.25	7.43	0.086	0.92
0.75	−5.91	6.03	0.264	0.86
0.95	−5.27	4.37	0.508	0.74
(c) 40 MPa				
0.05	1.1	23.9	−0.802	0.94
0.25	0.8	22.9	−1.47	0.93
0.5	1.08	22.4	−1.63	0.92
0.75	1.3	21.3	−1.65	0.9
0.95	1.92	19.9	−1.55	0.87

$$\frac{da}{dN} = \alpha_0(\Delta K)^{\alpha_1}(K_{max})^{\alpha_2}(R)^{\alpha_3}(K_{cl})^{\alpha_4}(f)^{\alpha_5}\ldots(X_n)^{\alpha_n} \qquad (7)$$

Now if the effects of strength are included, σ_u, and all the other specified variables in Eq. (6), one may obtain a single equation for the modeling of fatigue crack growth in the three types of concrete examined in this study. The results are presented in Table 5. The relative magnitudes of $\alpha_1, \alpha_2, \ldots, \alpha_5$ show the relative contributions of the specified variables to the overall fatigue crack growth rates. Hence, since α_1 is by far the largest single exponent (~10–11), this suggests that the overall fatigue crack growth rates are controlled largely by ΔK, and to

Table 5
Summary of complete multiparameter constants

$\ln(da/dN)$ *P*-level *Y*	Constant α_0	$ln(\Delta K)$ avg α_1	$\ln R$ α_2	ln Str α_3	Coefficient of correlation r^2
Table of regression coefficients without effect of strength					
0.05	−7.83	11.1	−0.479		0.975
0.25	−7.04	10.8	−0.671		0.976
0.5	−6.4	10.6	−0.708		0.967
0.75	−5.75	10.3	−0.754		0.946
0.95	−4.75	9.93	−0.76		0.9
Table of regression coefficients including effect of strength					
0.05	0	11.6	−0.321	−2.06	0.977
0.25	3.12	11.6	−0.465	−2.67	0.979
0.5	4.82	11.4	−0.481	−2.95	0.971
0.75	7.53	11.3	−0.486	−3.49	0.952
0.95	11.3	11.1	−0.435	−4.23	0.91

a lesser degree by the other variables. In any case, the average fatigue crack growth rates in the three types of concretes may be obtained by substituting the values of α_1 from Table 5 into Eq. (7), and taking natural logarithms. This gives:

$$\ln\left(\frac{da}{dN}\right)\Big|_{\phi} = 5.7 + 11.8\ln(\Delta K)_{avg} - 2.82\ln(\sigma_u) - 0.829\ln(K_{max}) + 0.583\ln(\phi) \quad (8)$$

$(r^2 = 0.989)$

where the above variables have their usual meaning.

The interdependencies between the different variables can be characterized by the Pearson correlation coefficient [11]. Examples of the correlation coefficients obtained from the current work are summarized in Table 6. These were obtained for the 30 MPa concrete that was tested at a stress ratio, R, of 0.1. The results show that all the variables are correlated to some degree. Furthermore, the variables need not be independent provided the Pearson correlation coefficients are determined for the specified variables are controlled largely by fatigue. Also, K_{max} or R are the second largest contributors (Table 5), although any one of these variables may mask out the influence of the other. Hence, it is recommended that either R or K_{max} be used in Eq. (6) or (8), and not both simultaneously.

4.4. Fatigue life prediction

The above multiparameter expressions are important since they provide a simple fracture mechanics framework for the prediction of fatigue crack growth rates at specified probability levels. In the simplest example, the fatigue crack growth associated with fatigue crack growth rates at specified probability level may be determined by the separation of variables and the numerical integration of Eq. (8). This gives:

$$\int_{a_0}^{a_c} da = \int_0^N \alpha_0(\Delta K)^{\alpha_1}(K_{max})^{\alpha_2}(\sigma_u)^{\alpha_4}(\phi)^{\alpha_5}\,dN \quad (9a)$$

or

$$\int_{a_0}^{a_c} da = \int_0^N \alpha_0(\Delta K)^{\alpha_1}(R)^{\alpha_3}(\sigma_u)^{\alpha_4}(\phi)^{\alpha_5}\,dN \quad (9b)$$

where a_0 is the initial crack length, a is the current crack length, N is the number of cycles and the other variables have their usual meaning. Eqs. (9a) and (9b) may be used to estimate crack growth for specified probability levels. For example, when $\phi = 0.5$, the predictions correspond to mean fits to the fatigue crack growth rate data. Predictions of a versus N obtained for crack growth at a stress ratio of 0.1 and values of ϕ of 0.05, 0.25, 0.50, 0.75 and 0.95 are presented in Fig. 5a–c, which were obtained from Eq. (9a) for concrete with strength levels, σ_u, of 30, 35 and 40 MPa, respectively. These show the expected trends, with crack length increasing with number of cycles and probability level.

Table 6
Summary of pearson correlation coefficients for multiparameter variables obtained from test at $R = 0.1$ on 30 MPa concrete

	$\ln(da/dN)$	$\ln(\Delta K)$	$\ln K_{max}$	$\ln P$-level
$\ln(da/dN)$	1			
$\ln(\Delta K)$	0.985	1		
$\ln K_{max}$	0.948	0.978	1	
$\ln P$-level	0.878	0.864	0.807	1

4.5. Implications

The implications of the above results are very significant. First, they show clearly how the model affects multiple variables within a single multiparameter expression that captures the effects of crack driving force parameters and occurrence probability. This reduces the problem of concrete life prediction to the numerical integration of a single equation for any specified occurrence probability level. It also incorporates a framework for choosing specific crack growth rate data in cases

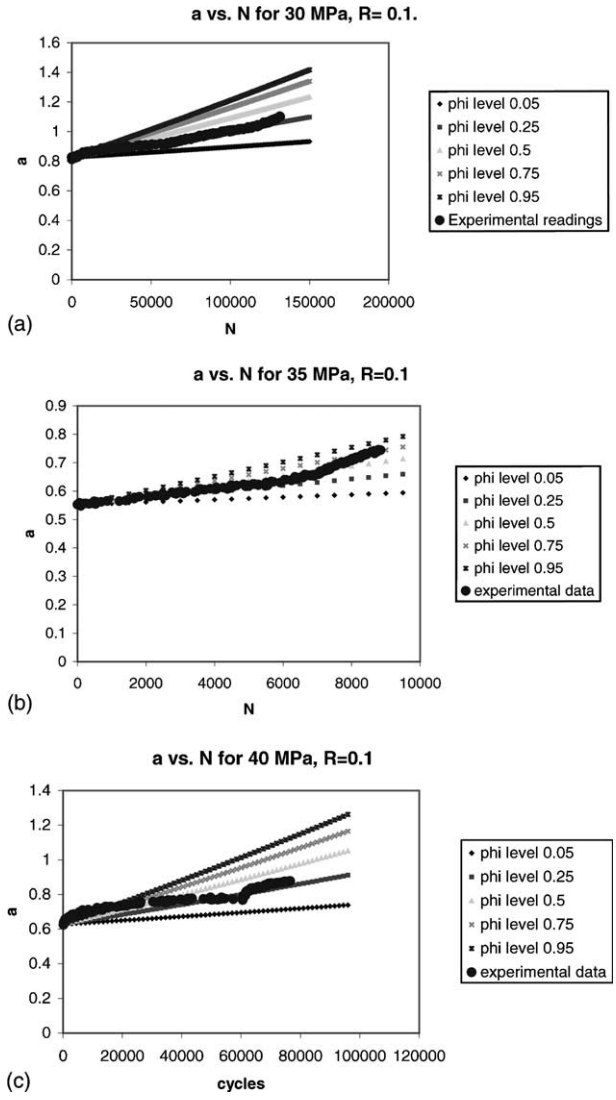

Fig. 5. Predictions of crack length versus number of cycles for specified occurrence probability levels in concrete with strength levels of: (a) 30 MPa, (b) 35 MPa and (c) 40 MPa. (All the tests were conducted at a stress ratio of 0.1.)

where the underlying heterogeneous structure contributes to large variabilities in the measured fatigue crack growth rate data. This is clearly so in the case of concrete.

One important consequence of the multiparameter framework is the natural incorporation of a size effect, as shown in Eq. (5). This provides an alternative approach to that of Bazant and Xu [7] for the modeling of the size effect in concrete. The relative magnitudes of the exponents of ΔK and size, S, also show that ΔK is the driving force for fatigue crack growth in concrete, although S provides an important secondary effect that should be modeled when sufficient experimental data are available. This was verified in the current study using the data of Bazant and Xu [7].

In addition to the effects of concrete size, the current work also provides a natural framework for the modeling of the effects of concrete strength. However, this should be done within a statistical framework, since the variability in the measured data is large. The occurrence probability provides a simple statistical measure that can be incorporated into multiparameter equations that include the effects of concrete strength, σ_u, stress ratio, R, maximum stress intensity factor, K_{max}, and the stress intensity factor range, ΔK (Eq. (6)). This was shown in the current work to be consistent with the experimental fatigue crack growth data obtained for the three grades of concrete that were examined.

Since the variability of the fatigue crack growth rate was relatively large, presumably a result of the heterogeneous nature of concrete materials that were studied, it is important to analyze fatigue crack growth in concrete within a probabilistic framework. This may be achieved by predicting as a function N for specified occurrence probability levels (Fig. 5), or by computing the material reliabilities or failure probabilities from measured p.d.f.s. that characterize the material variability. These functions may be derived using approaches presented in the preceding section for multiparameter fatigue crack growth problems. They provide the basis for the probabilistic modeling of fatigue crack growth in concrete and other materials. However, further work is needed to establish the general applicability of the current framework to other materials.

5. Conclusions

Fatigue crack growth has been studied in three grades of concrete with strength levels of 30, 35 and 40 MPa. The following conclusions have been reached from the combined experimental and theoretical study of the effects of multiple variables on fatigue crack growth in concrete:

1. A multiparameter equation can be used to relate the effects of multiple variables on fatigue crack growth in concrete. The power law expression, which is a logical extension of the Paris–Erdogan law, relates fatigue crack growth rate to stress intensity factor range, ΔK, maximum stress intensity factor, K_{max}, stress ratio, R, specimen size, S, ultimate strength, σ_u, and occurrence probability, ϕ.
2. The significant variabilities of the fatigue crack growth rates in the types of concrete assessed in this study are well characterized by log-normal distributions. These log-normal distributions may be used to rank the measured fatigue crack growth rate data in terms of occurrence probabilities that can be incorporated into a multiparameter framework.

6. Future work

A multiparameter framework can be used as the basis for the derivation of mathematical expressions for the prediction of material reliability (survival probability) or failure probabilities associated with fatigue crack growth in concrete. The probabilistic multiparameter framework would rely on the use of experimentally derived distributions of the material parameters C and m. Determining quantitatively, the nature of these distributions would enable the estimation of the survival and failure probabilities by means of simple mathematical expressions based on either observed crack lengths or known number of cycles undergone.

Acknowledgements

This research was supported by a research grant from the Division of Civil and Mechanical Systems of the National Science Foundation (NSF). Appreciation is extended to the Program Manager, Dr. Ken Chong. The authors are also grateful to Dr. Dan Davis, the initial NSF program monitor for his encouragement and support for the ideas behind the current work. The authors also would like to thank The Ohio State University and Princeton University for the use of the materials and testing facilities.

References

[1] Nonconventional concrete technologies, NMAB-484, National Materials Advisory Board. Washington, DC: National Academy Press; 1997.
[2] Nordby Gene M. Fatigue of concrete—a review of research. ACI J, Proc 1958;55(2):191–219.
[3] Marchand J, Pleau R, Gagne R. Deterioration of concrete due to freezing and thawing. In: Skalny J, Mindess S, editors. Material Science of Concrete IV, Acers. 1995. p. 283–354.
[4] Baluch MH, Quereshy AB, Azad AK. Fatigue crack propagation in plain concrete. In: Shah SP, Swartz SE, editors. Fracture of Concrete and Rock, SEM/RILEM International Conference, Houston, June 1987. New York: Springer-Verlag; 1989. p. 80–7.
[5] Ahmed TMA, Burley E, Rigden SR. Effect of alkali–silica reaction on the fatigue behavior of plain concrete tested in compression indirect tension and flexure. Mag Concr Res 1999;51:375–90.
[6] Raju K. Prestressed concrete. Tata McGraw Hill; 1994. p. 28–36.
[7] Bazant Z, Xu K. Size effect in fatigue fracture of concrete. ACI J 1991;88:390–9.
[8] Soboyejo ABO, Foster MA, Mercer C, Papritan JC, Soboyejo WO. A new multiparameter model for the prediction of fatigue crack growth in structural metallic materials. In: Paris PC, Jerina KL, editors. Fatigue and Fracture Mechanics, ASTM STP 1360, vol 30. West Conshohocken, PA: American Society for Testing of Materials; 1999.
[9] Soboyejo WO, Shen W, Lou J, Mercer C, Sinha V, Soboyejo ABO. A probabilistic framework for the modeling of fatigue in a lamella XD^{TM1} gamma titanium aluminide alloy. Int J Fatigue, 2002;24:69–81.
[10] Paris PC, Gomez M, Anderson WE. A rational analytical theory of fatigue. Trend Engng 1961;13:9–14.
[11] Ang AH-S, Tang WH. Probability concepts in engineering planning and design. John Wiley and Sons; 1975.